Geochemical Perspectives Letters

Sulfur and mercury MIF suggest volcanic contributions to Earth's atmosphere at 2.7 Ga

A.L. Zerkle[1*], M.W. Claire[1], T. Di Rocco[1,2], N.V. Grassineau[3], E.G. Nisbet[3], R. Sun[4], R. Yin[4*]

doi: 10.7185/geochemlet.2124

Abstract

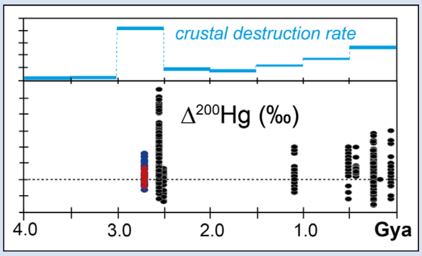

The Archean eon is associated with large-scale changes in Earth's geosphere and biosphere, including the onset of plate tectonics and the expansion of oxygenic photosynthesis, although the full impacts of these changes on the atmosphere remain unclear. Here we present coupled records of mass independent fractionation of sulfur (S-MIF) and mercury (Hg-MIF) isotopes from well preserved sediments of the ~2.7 billion year old (Ga) Manjeri Formation, Belingwe Greenstone Belt, Zimbabwe. These palaeoatmospheric proxies record different trends for S-MIF and odd number Hg-MIF *versus* even number Hg-MIF, providing novel constraints on atmospheric chemistry during this time. S-MIF and odd number Hg-MIF values are muted in comparison to values preserved in later Archean sediments, representing a combination of enhanced volcanic input and local mixing. Even number Hg-MIF is absent from these sediments, consistent with complete photo-oxidation of gaseous Hg^0, which could have been driven by increased halogen emissions from arc volcanism. When considered within a global geodynamic context, these MIF data suggest an important role for subduction zone-related volcanism associated with early plate tectonics in modulating the ~2.7 Ga atmosphere.

Received 5 May 2021 | Accepted 16 August 2021 | Published 9 September 2021

Introduction

The mid- to late-Archean, between ~3.2 and 2.5 billion years ago (Gyr), was a time of great transitions in Earth history, including the evolutionary proliferation of cyanobacteria performing oxygenic photosynthesis (Farquhar *et al.*, 2011; Nisbet and Fowler, 2014) and the development of plate tectonics (Hawkesworth *et al.*, 2020). Both of these events would have fundamentally altered Earth's surface environments and planetary habitability, the former by introducing a strong oxidant, and the latter by modulating fluxes of carbon and other volatile elements between the mantle and the surface (Zerkle, 2018). Although geosphere-biosphere-atmosphere feedbacks would have been essential in driving (and responding to) these critical changes in Earth's history, geochemical markers that place direct constraints on atmospheric evolution during this time period remain elusive.

Mass independent fractionation of sulfur isotopes (S-MIF) provide vital clues into past atmospheric chemistry. The presence of large magnitude S-MIF in rocks deposited prior to ~2.43 Ga provides compelling evidence for an oxygen-poor atmosphere in the Archean and early Palaeoproterozoic (Farquhar *et al.*, 2000; Warke *et al.*, 2020). The S-MIF record also displays significant variations in magnitude, sign, and quadruple S isotope systematics (expressed as Δ^{33}S and Δ^{36}S; Eqs. S-2, S-3) that could provide additional constraints on Earth's reducing atmosphere. In particular, a decrease in the magnitude of S-MIF has been reported in Archean rocks deposited between ~3.2 and 2.7 Ga (Fig. 1). This "mid-Archean MIF minimum" has been variably attributed to changes in global atmospheric chemistry, which could shield or dampen S-MIF forming reactions (Farquhar *et al.*, 2007; Domagal-Goldman *et al.*, 2008; Kurzweil *et al.*, 2013; Liu *et al.*, 2019), or to dilution or mixing of atmospheric sulfur sources on a local or regional scale (Guy *et al.*, 2012; Thomazo *et al.*, 2013; Marin-Carbonne *et al.*, 2014).

MIF of mercury (Hg) isotopes in marine sediments can provide additional constraints on atmospheric chemistry. Mercury undergoes MIF of both odd number isotopes (expressed as Δ^{199}Hg and Δ^{201}Hg; Eq. S-5) and even number isotopes (expressed as Δ^{200}Hg) during Hg transformations between the atmosphere and oceans (Blum *et al.*, 2014). Odd number Hg-MIF is predominatly produced by photo-reduction of aqueous Hg^{2+}, which occurs mainly in the surface ocean but also in rain droplets (Bergquist and Blum, 2007). By contrast, even number Hg-MIF is only produced during gas phase Hg^0 photo-oxidation in the atmosphere (Cai and Chen, 2016). In the oceans, MIF-bearing Hg complexes with organic matter and sulfur ligands and is deposited in the sediments. The resulting Hg-MIF signals are robust to post-depositional alteration (Grasby *et al.*, 2016) and can record additional, complementary atmospheric constraints (Zerkle *et al.*, 2020). Here we present coupled records

1. School of Earth and Environmental Sciences and Centre for Exoplanet Science, University of St Andrews, St Andrews, Fife, KY16 9AL, Scotland, UK
2. Current address: Geowissenschaftliches Zentrum, Universität Göttingen, 37077 Göttingen, Germany
3. Department of Earth Sciences, Royal Holloway, University of London, Egham TW20 OEX, UK
4. State Key Laboratory of Ore Deposit Geochemistry, Institute of Geochemistry, Chinese Academy of Sciences, Guiyang 550081, China
* Corresponding author (email: az29@st-andrews.ac.uk, yinrunsheng@mail.gyig.ac.cn)

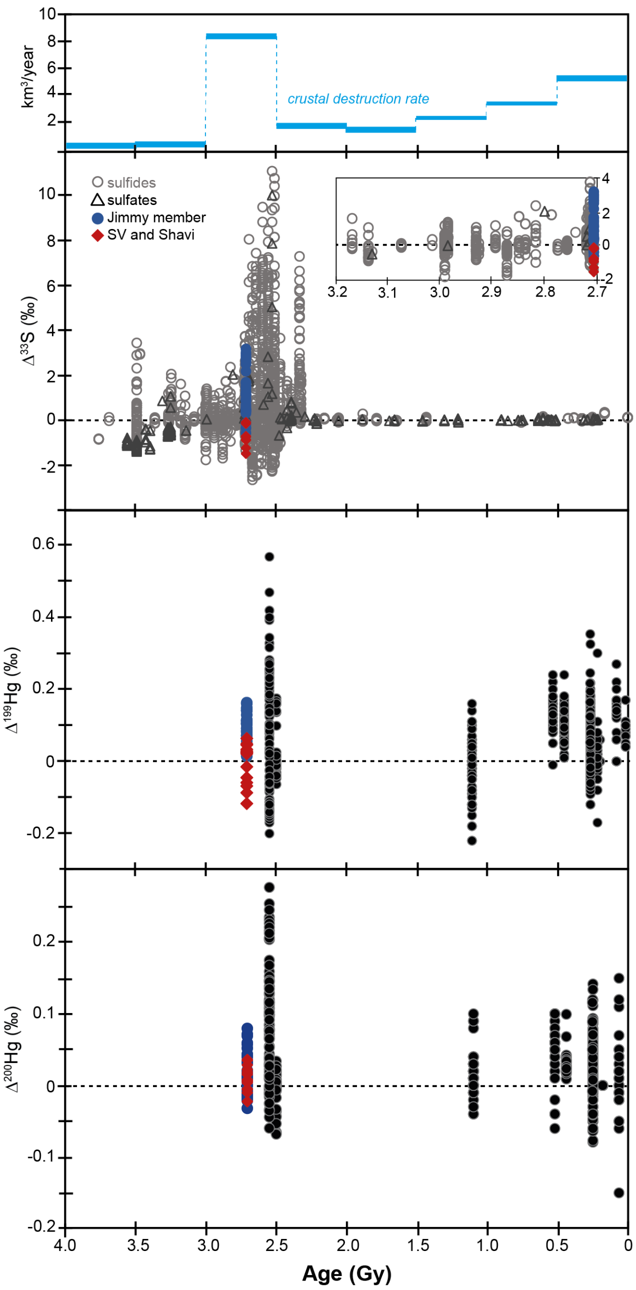

Figure 1 Temporal trends in S-MIF and Hg-MIF through time (updated from Farquhar *et al.*, 2014, and Zerkle *et al.*, 2020). Crustal destruction rates are modelled for 500 million year bins (Dhuime *et al.*, 2018).

of S-MIF and Hg-MIF data from well preserved sediments of the ~2.7 Ga Manjeri Formation of the Belingwe Greenstone Belt, Zimbabwe, to determine local *versus* global controls on MIF records, and to unravel drivers of Archean atmospheric chemistry.

Sulfur and Mercury MIF in the Manjeri Formation

Our samples were collected from three drill cores through the ~2.7 Ga Manjeri Formation (Fm) of the Belingwe Greenstone Belt, Zimbabwe (as detailed in Yang *et al.*, 2019, and SI). This section of the Manjeri Fm (Hunter *et al.*, 1998) records a marine transgression from a basal unconformity and the intertidal facies of the Spring Valley (SV) member, through the subtidal Shavi member (preserved in the NERCMAR core) to the deeper water shales of the Jimmy member (preserved in cores A and B).

S-MIF from the Manjeri Fm had Δ^{33}S values ranging from -1.5 to +3.1 ‰, with positive Δ^{33}S values dominating the Jimmy member and negative Δ^{33}S values dominating the Spring Valley and Shavi members (Fig. 2). These S-MIF values are larger in magnitude than bulk rock Δ^{33}S values previously reported from ~2.7 Ga (*e.g.*, Thomazo *et al.*, 2013), but still significantly smaller than Δ^{33}S values preserved in ~2.5 Ga sediments (Fig. 1). Shielding of S-MIF forming reactions by oxygen or organic haze have been proposed to erase or decrease S-MIF (Domagal-Goldman *et al.*, 2008; Kurzweil *et al.*, 2013; Liu *et al.*, 2019), but the persistence of S-MIF in these samples precludes an ozone layer, and the Δ^{36}S-Δ^{33}S dynamics are inconsistent with haze formation (Fig. 2b) (Zerkle *et al.*, 2012). Modelling studies have shown that higher total volcanic sulfur fluxes can alter sulfur exit channels and decrease S-MIF values (Claire *et al.*, 2014), providing one potential explanation for lower magnitude atmospheric S-MIF.

Local- or basinal-scale mixing of primary atmospheric S sources can further dampen sedimentary S-MIF signals (*e.g.*, Marin-Carbonne *et al.*, 2014). Following mass balance, the preservation of S-MIF in ancient sediments requires two or more exit channels for atmospheric sulfur, conventionally considered to be elemental sulfur carrying a positive Δ^{33}S signature (as seen in the Jimmy member) and sulfate carrying a negative Δ^{33}S signal (as seen in the SV and Shavi members), although this remains debated (Claire *et al.*, 2014; Harman *et al.*, 2018). In particular, the very small S-MIF in some samples from the Jimmy member (with $\Delta^{33}S < 2$ ‰) could reflect further muting of primary atmospheric S-MIF values *via* mixing. Mixing could have been driven by biological processes (*e.g.*, through re-oxidation of reduced S), physical processes (*e.g.*, mixing of Fe-sulfides derived from sulfate reduction with polysulfides to form pyrite), or some combination of both (Fig. 2a). Previous studies indicate that Jimmy member sediments supported an active biogeochemical S cycle in proximity to a redox interface (Yang *et al.*, 2019), consistent with this interpretation.

Mercury isotopes provide new insights into environmental conditions during deposition of the Manjeri strata. δ^{202}Hg values alone are difficult to interpret, since mass dependent fractionation of Hg occurs during all Hg cycling processes (Blum *et al.*, 2014). In contrast, mercury MIF provides clearer constraints on atmospheric Hg cycling, as it mainly occurs during photon-mediated processes with little contribution from biogeochemical cycling, and even number Hg-MIF is produced exclusively in the atmosphere. Odd number Hg-MIF from the Manjeri Fm support two sources of Hg to the sediments, one dominated by positive odd number Hg-MIF, and one dominated by negative odd number Hg-MIF (Fig. 2c). In the modern environment, rain and open marine samples that mainly contain Hg^{2+} species are characterised by positive odd number Hg-MIF (*e.g.*, Štrok *et al.*, 2015), while terrestrial reservoirs and modern coastal sediments that primarily accumulate Hg^0 are characterised by negative odd number Hg-MIF (Blum *et al.*, 2014). These Hg-MIF values therefore suggest that the dominant source of Hg to the SV and Shavi members was Hg^0 species deposited in a shallow depositional environment, where enhanced terrestrial nutrient input stimulated local primary productivity, driving near shore anoxia. The Jimmy member, on the other hand, was dominated by Hg^{2+} species deposited in a more oligotrophic open ocean environment, adjacent to a deeper water chemocline. This depositional scenario is supported by previously published sedimentology (Hunter *et al.*, 1998) and ocean redox data from these same cores (Yang *et al.*, 2019). Combined S-MIF and

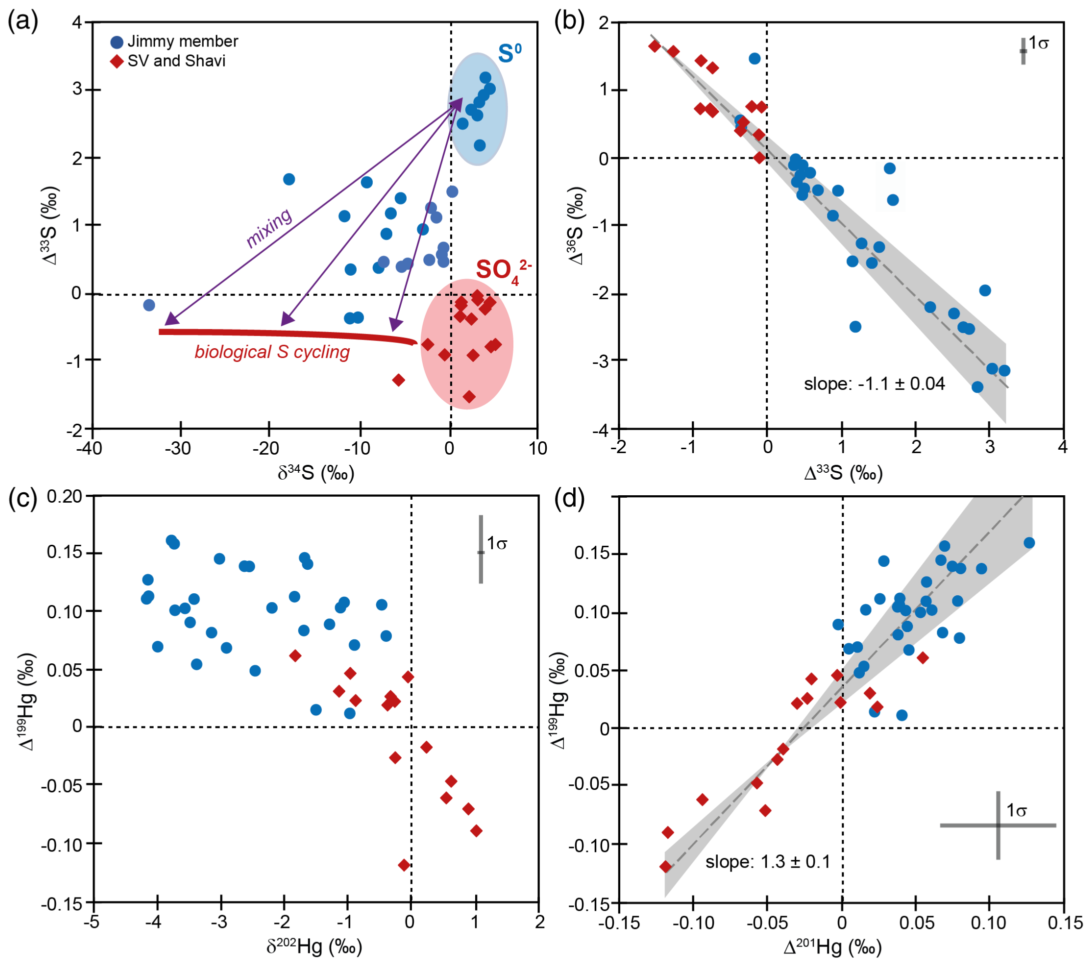

Figure 2 **(a-d)** Cross plots of S-MIF and Hg-MIF values. Panel **(a)** includes interpretations of S-MIF based on the conventional view of sulfur exit channels (but see Harman *et al.*, 2018, for an alternative view). Panels **(b)** and **(d)** include orthogonal data regressions, showing the calculated linear slopes (gray dashed line) and 3σ confidence intervals (gray blue area). The Δ^{36}S/Δ^{33}S slope is consistent with the Archean reference array (Ono *et al.*, 2009); the Δ^{199}Hg/Δ^{201}Hg slope is consistent with production of odd number Hg-MIF during Hg^{2+} photo-reduction (Bergquist and Blum, 2007).

Hg-MIF data also indicate that the atmospheric exit channel carrying a negative Δ^{33}S signal dominated the S pool in shallow, near shore environments, while atmospheric S carrying a positive Δ^{33}S signal dominated in open ocean environments (Fig. 3).

Similar to S-MIF, Hg-MIF values from the 2.7 Ga Belingwe strata are muted (odd number Hg-MIF) or completely absent (even number Hg-MIF) in comparison to Hg-MIF data from the later Archean (Fig. 1). A decrease in the magnitude of sedimentary Hg-MIF towards values of 0 ‰ is generally attributed to enhanced atmospheric flux of vocanically-derived Hg^0 to the sediments, since volcanic Hg^0 has Δ^{199}Hg and Δ^{200}Hg values of 0 ‰ (Zambardi *et al.*, 2009). Ratios of mercury to TOC in the Manjeri Fm support high volcanic Hg^0 inputs to the sediments, particularly in the near shore SV and Shavi members (1274 ± 584 ppb Hg/wt. % TOC; Grasby *et al.*, 2019). However, volcanic Hg^0 input would affect both odd number and even number Hg-MIF similarly, as would any post-depositional mixing processes, so neither of these mechanisms can explain the entirety of our Hg-MIF data.

The complete absence of even number Hg-MIF in these sediments instead requires further alteration of the photo-oxidation processes that uniquely produce Δ^{200}Hg anomalies. The dominant oxidation pathway for Hg^0 in the modern atmosphere is reaction with halogens, such as bromine and chlorine (Dibble *et al.*, 2020), and these reactions have been shown to produce

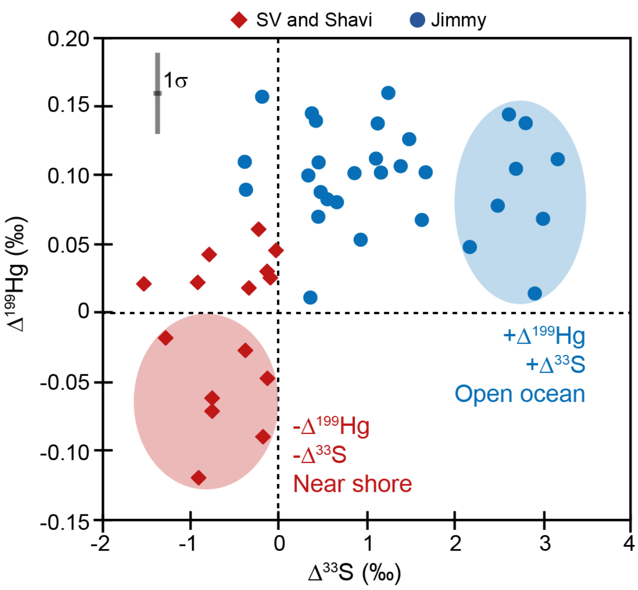

Figure 3 Trends in S-MIF *versus* Hg-MIF, with associated interpretations based on comparison with modern sedimentary Hg-MIF values.

even number Hg-MIF (Sun *et al.*, 2016). In the modern Earth system, the largest volcanic source of halogens is from subduction zone-related arc volcanism (Pyle and Mather, 2009). Enhanced volcanic fluxes of SO_2 and halogens into the atmosphere could have driven Hg^0 photo-oxidation reactions near to completion, as seen with seasonal atmospheric mercury depletion events that occur in modern polar regions (Carignan and Sonke, 2010), erasing any even number Hg-MIF signal. Halogens could have additionally been supplied from komatiitic volcanism, as indicated by the overlying Zeederbers Fm deposited several million years later (Cameron *et al.*, 1979).

Enhanced global volcanic gas fluxes could have contributed both MIF-free sulfur and mercury to the sediments, diluting the overall magnitudes of sedimentary MIF. In addition, the complete lack of even number Hg-MIF in these sediments suggests a volcanic source rich in halogens, similar to modern arc volcanism. Therefore, enhanced arc volcanism provides the only self-consistent mechanism that can reconcile all three sets of MIF records. Within a global geodynamic context, models of continental crust formation suggest that crustal destruction rates increased dramatically at ~3.0 Ga, inferred to represent the widespread development of subduction zones (Fig. 1) (Dhuime *et al.*, 2018). The increase in crustal destruction rates, coupled with the development and amalgamation of Archean supercontinents, are taken to reflect the onset of plate tectonics as the dominant global regime during this time (Hawkesworth *et al.*, 2020). Our data are consistent with enhanced volatile fluxes from subduction zone arc volcanism at ~2.7 Ga. Following this scenario, the increase in S-MIF and Hg-MIF between 2.7 and 2.5 Ga could be explained by decreased volcanic emissions during the transition to tectonic quiescence in the Palaeoproterozoic (Cawood and Hawkesworth, 2014). As a corollary, the time span of the mid-Archean S-MIF minimum could indicate that volcanic emissions from plate tectonics exerted a fundamental control on atmospheric chemistry from ~3.2 to 2.7 Ga, before biology wrested control in the ensuing ~200 million years (*e.g.*, Kurzweil *et al.*, 2013; Izon *et al.*, 2017).

Acknowledgements

This study received funding from a Natural Environment Research Council Standard Grant NE/M001156/1 (ALZ, EGN), and from the European Research Council under the European Union's Horizon 2020 research and innovation programme (Grant 678812 to MWC). RS and RY were supported by the Natural Science Foundation of China (41873047).

Editor: Gavin Foster

Additional Information

Supplementary Information accompanies this letter at https://www.geochemicalperspectivesletters.org/article2124.

Cite this letter as: Zerkle, A.L., Claire, M.W., Di Rocco, T., Grassineau, N.V., Nisbet, E.G., Sun, R., Yin, R. (2021) Sulfur and mercury MIF suggest volcanic contributions to Earth's atmosphere at 2.7 Ga. *Geochem. Persp. Let.* 18, 48–52.

References

Bergquist, B.A., Blum, J.D. (2007) Mass-dependent and -independent fractionation of Hg isotopes by photoreduction in aquatic systems. *Science* 318, 417–420.

Blum, J.D., Sherman, L.S., Johnson, M.W. (2014) Mercury isotopes in earth and environmental sciences. *Annual Review of Earth and Planetary Sciences* 42, 249–269.

Cai, H.M., Chen, J.B. (2016) Mass-independent fractionation of even mercury isotopes. *Science Bulletin* 61, 116–124.

Cameron, W.E., Nisbet, E.G., Dietrich, V.J. (1979) Boninites, komatiites, and ophiolitic basalts. *Nature* 280.

Carignan, J., Sonke, J.E. (2010) The effect of atmospheric mercury depletion events on the net deposition flux around Hudson Bay, Canada. *Atmospheric Environment* 44, 4372–4379.

Cawood, P.A., Hawkesworth, C.J. (2014) Earth's middle age. *Geology* 42, 503–506.

Claire, M.W., Kasting, J.F., Domagal-Goldman, S.D., Stueken, E.E., Buick, R., Meadows, V.S. (2014) Modeling the signature of sulfur mass-independent fractionation produced in the Archean atmosphere. *Geochimica et Cosmochimica Acta* 141, 365–380.

Dhuime, B., Hawkesworth, C.J., Delavault, H., Cawood, P.A. (2018) Rates of generation and destruction of the continental crust: implications for continental growth. *Philosophical Transactions of the Royal Society A* 376.

Dibble, T.S., Tetu, H.L., Jiao, Y.G., Thackray, C.P., Jacob, D.J. (2020) Modeling the OH-Initiated Oxidation of Mercury in the Global Atmosphere without Violating Physical Laws. *Journal of Physical Chemistry A* 124, 444–453.

Domagal-Goldman, S.D., Kasting, J.F., Johnston, D.T., Farquhar, J. (2008) Organic haze, glaciations and multiple sulfur isotopes in the Mid-Archean Era. *Earth and Planetary Science Letters* 269, 29–40.

Farquhar, J., Bao, H.M., Thiemens, M. (2000) Atmospheric influence of Earth's earliest sulfur cycle. *Science* 289, 756–758.

Farquhar, J., Peters, M., Johnston, D.T., Strauss, H., Masterson, A., Wiechert, U., Kaufman, A.J. (2007) Isotopic evidence for Mesoarchaean anoxia and changing atmospheric sulphur chemistry. *Nature* 449, 706–709.

Farquhar, J., Zerkle, A.L., Bekker, A. (2011) Geological constraints on the origin of oxygenic photosynthesis. *Photosynthesis Research* 107, 11–36.

Farquhar, J., Zerkle, A.L., Bekker, A. (2014) 6.4 - Geologic and Geochemical Constraints on the Earth's Early Atmosphere. In: Holland, H.D., Turekian, K.K. (Eds.) *Treatise on Geochemistry*. Second Edition, Elsevier, Oxford, 91–138.

Grasby, S.E., Shen, W., Yin, R., Gleason, J.D., Blum, J.D., Lepak, R.F., Hurley, J.P., Beauchamp, B. (2016) Isotopic signatures of mercury contamination in latest Permian oceans. *Geology* 45, 55–58.

Grasby, S.E., Them II, T.R., Chen, Z., Yin, R., Ardakani, O.H. (2019) Mercury as a proxy for volcanic emmisions in the geologic record. *Earth Science Reviews* 196, 102880.

Guy, B.M., Ono, S., Gutzmer, J., Kaufman, A., Lin, Y., Fogel, M., Beukes, N. (2012) A multiple sulfur and organic carbon isotope record from non-conglomeratic sedimentary rocks of the Mesoarchean Witwatersrand Supergroup, South Africa. *Precambrian Research* 216-219, 208–231.

Harman, C.E., Pavlov, A., Babikov, D., Kasting, J.F. (2018) Chain formation as a mechanism for mass-independent fractionation of sulfur isotopes in the Archean atmosphere. *Earth and Planetary Science Letters* 496, 238–247.

Hawkesworth, C.J., Cawood, P.A., Dhuime, B. (2020) The evolution of the continental crust and the onset of plate tectonics. *Frontiers in Earth Science* 8.

Hunter, M.A., Bickle, M.J., Nisbet, E.G., Martin, A., Chapman, H.J. (1998) Continental extensional setting for the Archean Belingwe Greenstone Belt, Zimbabwe. *Geology* 26, 883–886.

Izon, G., Zerkle, A.L., Williford, K.H., Farquhar, J., Poulton, S.W., Claire, M.W. (2017) Biological regulation of atmospheric chemistry en route to planetary oxygenation. *PNAS* 114, 2571–2579.

Kurzweil, F., Claire, M.W., Thomazo, C., Peters, M., Hannington, M.D., Strauss, H. (2013) Atmospheric sulfur rearrangement 2.7 billion years ago: Evidence for oxygenic photosynthesis. *Earth and Planetary Science Letters* 366, 17–26.

Liu, P., Harman, C.E., Kasting, J.F., Hu, Y., Wang, J. (2019) Can organic haze and O2 plumes explain patterns of sulfur mass-independent fractionation during the Archean? *Earth and Planetary Science Letters* 526, 115767.

Marin-Carbonne, J., Rollion-Bard, C., Bekker, A., Rouxel, O., Agangi, A., Cavalazzi, B., Wohlgemuth-Ueberwasser, C.C., Hofmann, A., McKeegan, K.D. (2014) Coupled Fe and S isotope variations in pyrite nodules from Archean shale. *Earth and Planetary Science Letters* 392, 67–79.

Nisbet, E.G., Fowler, C.M.R. (2014) 10.1 - The Early History of Life. In: Holland, H.D., Turekian, K.K. (Eds.) *Treatise on Geochemistry*. Second Edition, Elsevier, Oxford, 1–42.

Ono, S., Beukes, N.J., Rumble, D. (2009) Origin of two distinct multiple-sulfur isotope compositions of pyrite in the 2.5 Ga Klein Naute Formation, Griqualand West Basin, South Afric. *Precambrian Research* 169, 48–57.

Pyle, D.M., Mather, T.A. (2009) Halogens in igneous processes and their fluxes to the atmosphere and oceans from volcanic activity: A review. *Chemical Geology* 263, 110–121.

Štrok, M., Baya, P.A., Hintelmann, H. (2015) The mercury isotope composition of Arctic coastal seawater. *Comptes Rendus Geoscience* 347, 368–376.

Sun, G., Sommar, J., Feng, X., Lin, C.-J., Ge, M., Wang, W., Yin, R., Fu, X., Shang, L. (2016) Mass-dependent and independent fractionation of mercury isotopes during gas-phase oxidation of elemental mercury vapor by atomic Cl and Br. *Environmental Science & Technology* 50, 9232–9241.

Thomazo, C., Grassineau, N.V., Nisbet, E.G., Peters, M., Strauss, H. (2013) Multiple sulfur and carbon isotope composition of sediments from the Belingwe Greenstone Belt (Zimbabwe): A biogenic methane regulation on mass independent fractionation of sulfur during the Neoarchean? *Geochimica et Cosmochimica Acta* 121, 120–138.

Warke, M.R., Di Rocco, T., Zerkle, A.L., Lepland, A., Prave, A.R., Martin, A., Ueno, Y., Condon, D.J., Claire, M. (2020) The Great Oxidation Event preceded a Paleoproterozoic "snowball Earth". *PNAS* 117, 13314–13320.

Yang, J., Junium, C.K., Grassineau, N.V., Nisbet, E.G., Izon, G., Mettam, C., Martin, A., Zerkle, A.L. (2019) Ammonium availability in the Late Archaean nitrogen cycle. *Nature Geoscience* 12, 553–557.

Zambardi, T., Sonke, J.E., Toutain, J.P., Sortino, F., Shinohara, H. (2009) Mercury emissions and stable isotopic compositions at Vulcano Island (Italy). *Earth and Planetary Science Letters* 277, 236–243.

Zerkle, A.L. (2018) Biogeodynamics: bridging the gap between surface and deep Earth processes. *Philosophical Transactions of the Royal Society A* 376, 20170401.

Zerkle, A.L., Claire, M.W., Domagal-Goldman, S.D., Farquhar, J., Poulton, S.W. (2012) A bistable organic-rich atmosphere on the Neoarchean Earth. *Nature Geoscience* 5, 359–363.

Zerkle, A.L., Yin, R., Chen, C., Li, X., Izon, G., Grasby, S. (2020) Anomalous fractionation of mercury isotopes in the Late Archean atmosphere. *Nature Communications* 11, 1709.